RESEARCH ARTICLE
Available Online at *http://www.aer-journal.info*

Aqueous Fluoride Rapid Detection based on TBAF Desilylation by a Novel Fluorogenic 7-O-tert-butyldimethylsylyl-2-(hydroxyimino)-4-methyl-2*H*-chromene-3-carbonitrile

E. O. Akumu*[1,2], S. Barasa[1], S. Lutta[1] and T. Akeng'a[1]

[1]*Department of Chemistry and Biochemistry, University of Eldoret, P. O. Box 1125-30100, Eldoret-Kenya*

[2]*Department of Physical and Biological Sciences, Kabarak University, Private Bag-20157, Kabarak-Kenya*

*Corresponding Author's E-mail: oakumu@kabarak.ac.ke

Abstract

This report illustrates the synthesis and properties of a novel fluoride detector also called 7-O-tert-butyldimethylsylyl-2-(hydroxyimino)-4-methyl-2H-chromene-3-carbonitrile, which emits a lavender blue fluorescence in aqueous solution when fluoride ions are present. Bk-F93 F2000 Fluorospectrophotometer (FS), MRC-UV-Vis Spectrophotometer-UV-(11S/N; UEB1011006), GC micromass spectrometer (Micromass, Wythenshawe, Waters, Inc. UK), and Bruker Avance NEO 400 MHz (TXO cryogenic probe) NMR spectrometers were used for the spectral study. MestreNova (v14.0.0) program was used to process the NMR spectra. This sensor is highly specific and sensitive to water - soluble fluoride. The findings also show that fluoride doses as minimal as 0.19 μM (3.61 x10^{11} mgL^{-1}) and 8.5 μM (3.79x10^{10} mgL^{-1}) in tetra-n-butylammonium fluoride (TBAF) and sodium fluoride (NaF) respectively can be reliably measured almost immediately, as shown by 2nd order rate constant of 1.4 x10 $M^{-1}min^{-1}$, in comparison to most fluoride sensors' range of 0.54 - 116$M^{-1}min^{-1}$. The synthetic compound's responsiveness as a fluoride probe in chloride, bromide, iodide, nitrate and sulfate rich water indicated no direct detection interference by any of evaluated ionic species. The quantum yield of this synthesized probe was established to be higher than the selected standard (quinine sulfphate), with values at 0.72 and 0.54 respectively. Fluoride screening with 7-O-tert-butyldimethylsylyl-2-(hydroxyimino)-4-methyl-2H-chromene-3-carbonitrile is simple and fast compared to conventional approaches that involve professional staff. As a result, the approach outlined herein is applicable and incredibly useful for assessing the quality of potable water in communities.

Keywords: Fluoride, Sensor, Potable Water, 7-O-tert-butyldimethylsylyl-2-(hydroxyimino)-4-methyl-2*H*-chromene-3-carbonitrile

INTRODUCTION

Numerous methods of analysis for the recognition and estimation of ions have been established during the last few decades (Xu *et al.,* 2020). Relatively simple approaches, such as colorimetric (Wu *et al.,* 2020) and fluorescence-based (Ullah *et al.,* 2021) approaches, have gotten a lot of coverage due to their ease of use, consistency, and relatively low cost.

Fluoride (F–) ions are essential in several metabolic processes (Keesari *et al.*, 2021), including water fluoridation (Song & Kim 2021), oral hygiene (Kruse *et al.*, 2021) and

bone disease management (Helte *et al.*, 2021). As a result, highly sensitive and specific fluoride identification is important. Because of their widespread use in biochemical and environmental processes, sensitive optical probes, particularly fluoride fluorescent probes have piqued the interest of researchers.

Due to the negative involvement in various forms of fluorosis and medical care in osteoporosis, chemosensors for fluoride ion identification have earned a lot more interest. Chronic F- ion deficiency or excess causes dental and skeletal fluorosis (Kabir *et al*., 2020), gastric(Akimov & Kostenko 2020) and kidney defects, urolithiasis, and even mortality in humans(Kabir *et al.,* 2020). The World Health Organization recommends 1.5 mg/L of fluoride ion in drinking water to be an optimal dose (Srivastava, 2020).

Förster or fluorescence resonance energy transfer (FRET) (Mizuta *et al.,* 2021), intramolecular charge transfer (ICT) (Liese & Haberhauer 2018), and photoinduced electron transfer (PET) (Magri, 2021) based fluoride chemosensors have been developed over years. The ability of molecules with functional groups such as urea/thiourea (Cao *et al.,* 2018), amide (Yeung *et al.,* 2014), guanidinium and ammonium derivatives (Mohanasundaram *et al.,* 2020) to identify fluoride ions through electrostatic H-bond interactions. These sensors have a wide range of applications in both biological as well as chemical processes. In pursuit the development of an efficient fluoride ion detector and tracking probe, we present a basic and yet incredibly effective sensor based on cyanocoumarin (Figure 1). When tested using chromogenic and fluorometric approaches, this compound was able to selectively detect F- in the presence of other Fluoride-competing anions. This detection is based on intramolecular charge transfer mechanism (Figure 2).
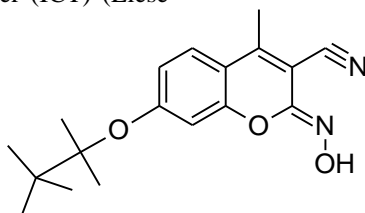

Figure 1: 3-cyano-7-hydroxy-4-methylcoumarin **(1)**

Figure 2: Charge transfer mechanism.

METHODS
List of Chemicals Used
1,4-Dioxane anhydrous) - Sigma-Aldrich, 99.8%

3-cyano-4-methylcoumarin (Sigma-Aldrich 97%)

4-(2-Hydroxyethyl) piperazine-1-ethanesulfonic acid (HEPES) 1 M in H_2O

cetyltrimethylammonium bromide, (CTAB) - Sigma-Aldrich Calbiochem® 98%

Dichloromethane (DCM) - AR

Hydroxylamine hydrochloride ($NH_2OH.HCl$) – AR/ACS 99%

Imidazole (Sigma-Aldrich 99.5%)

Silica gel 60 (230-400 mesh) and G-HR for TLC

Sodium hydroxide (NaOH) - Sigma-Aldrich Analytical, Puriss

Sodium nitrate, analytical standard,

Anhydrous sodium sulfate powder- ACS reagent, ≥99.0%,

Tert-butyldimethylsilylchloride (TBDPSCl) - Sigma-Aldrich 97%

Tetrahydrofuran (THF) - AR

Tetra-n-butylammonium bromide (TBAB) - Sigma-Aldrich 97%

Tetra-n-butylammonium chloride (TBAC) - Sigma-Aldrich 97%

Tetra-n-butylammonium fluoride (TBAF) - Sigma-Aldrich 97%

TLC Silica gel 60 F_{254} (Merck, Darmstadt, Germany) on pre-coated Aluminium sheets

Characterization Techniques Used
The characterization techno=iques applied in this work include: UV-Vis spectroscopy (MRC-UV-Vis Spectrophotometer-UV-(11S/N; UEB1011006) and UV-lamp - UV303$_D$); Fluorescence spectroscopy (Bk-F93 F2000 Fluorospectrophotometer); Mass spectrometry (GC micromass spectrometer - Micromass, Wythenshawe, Waters, Inc. UK) and NMR spectroscopy (Bruker Avance NEO 500 MHz TXO cryogenic probe NMR spectrometer and MestreNova (v14.0.0) software).

Synthesis of Compound 3:7-O-tert-butyldimethylsylyl-2-(hydroxyimino)-4-methyl-2*H*-chromene-3-carbonitrile
Compound (**2**) was synthesized by introducing a fluoride responsive butyldimethylsilyl (TBDMS) moiety into 3-cyano-7-hydroxy-4-methylcoumarin (**1**) as earlier reported. A solution of 6.3 g (0.02 moles) of compound (**2**) in 200 mL mixture of Tetrahydrofuran (THF) and dry dichloromethane (DCM) in the ratio of (1:3) was made in the presence of nitrogen gas. 1.4 g (0.02 moles) of hydroxylamine hydrochloride (NH$_2$OH.HCl) was dissolved in 100 mL of distilled and de-ionized H$_2$O to yield a different solution. The aqueous NH$_2$OH.HCl was added to a solution containing compound (**2**). A glass rod was used to stir themixture until until clear. 0.8 g (0.02 moles) of NaOH dissolved in 100 mL of distilled and de-ionized H$_2$O was then added to this solution and further stirred until clear. The solution was then added to the mixture in the reagent bottle and allowed to shake for twelve hours. This was followed by using a Whatman filter paper. The non-polar portion then was exposed to anhydrous sodium sulphate (Na$_2$SO$_4$) to dry. The sample was then filtered and concentrated by use a Büchi rotavapour at a lower temperature and pressure to yield a crude sample. Column chromatography was used to progressively purify the samples using differing proportions of DCM: THF as the moving solvent. At this stage, the product was a bright yellow crystalline solid. These crystals were purified once more in a column but use of DCM: THF solvent mixture. Only the central parts of the fractions were picked and concentrated during the second column purification. This product was purified further using preparative thin layer chromatography in a DCM: THF solvent mixrure in the ratio of 1:3. The extracted mass was (2.59 g) with a percentage yield of 41.1%. Figure 2 gives an illustration of how compound (**3**) was synthesized.
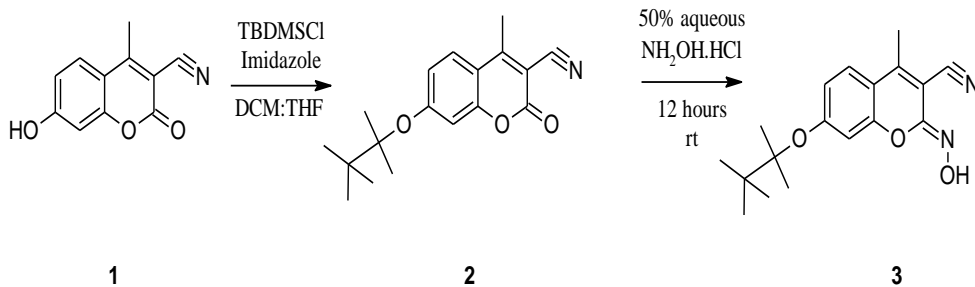
Figure 2: Schematic for the synthesis of compounds (**3**).

Fluorescence Fluoride Testing

The activity of 7-O-tert-butyldimethylsylyl-2-(hydroxyimino)-4-methyl-2H-chromene-3-carbonitrile (**3**) and fluoride ions (Figure 3) in dioxane solution was investigated using colorimetric and fluorescent methods. An aqueous TBAF dosage range of between 0.1-100 mg of the sensor in 100 ml solution was made. 1 mL of a 4 % compound (**3**) dioxane solution was applied to each of these solutions. These solutions were incubated for 15 minutes at room temperature (rt) in a 1:1 (v/v) solution of 10 mM HEPES (pH = 7.4):dioxane. The fluorescence spectra for each of the TBAF dosages were recorded with excitation and emission wavelengths of 332 nm and 360 nm, respectively.
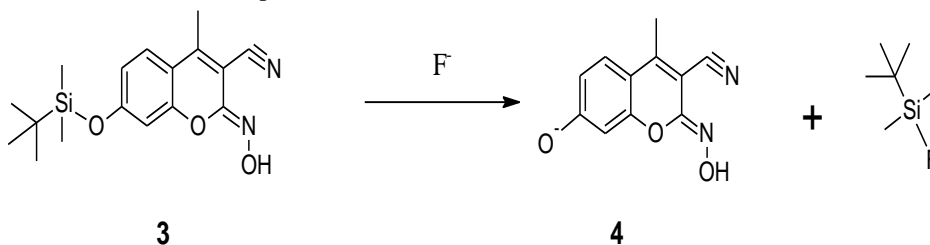

Figure 3: Schematic of desilylation of compound (**3**).

Selectivity Studies

Variable concentrations of the chosen anions were prepared, namely chloride, bromide, iodide, nitrate, and sulphate (all at 200 μM), as well as TBAF and NaF (both at 200 μM). The experiments were carried out in a solution with a pH sustained at 7.4 by a 1:1 (v/v) 10 mM mixture HEPES in dioxane. 1 mL of a 4 % solution of the synthesized compound contained in dioxane was then added to 40 mL of the ionic test samples. These solutions were incubated for 20 minutes at rt. Fluorescence studies in terms of absorption and emission frequencies were done for each of these solutions. Three replicates were tested for each anion.

Quantum Yield Measurements

In order to prevent self-quenching, the absorbance was maintained at ≤0.05 during quantum yield measurements. The fluorescence intensity was measured at the excitation frequency. The quantum yield on fluorescence for compound **3** + F- was determined using equation (i).

$$\Phi_X = \Phi_{ST}\left(\frac{Grad_x}{Grad_{ST}}\right)\left(\frac{\eta_x^2}{\eta_{ST}^2}\right)\ldots\ldots\ldots(i)$$

Where;
Φ_{ST} = quantum yield of standard
Φ_x = quantum yield of sample
η = solvent refractive index
$Grad_X$ = sample gradient.
$Grad_{ST}$ = standard gradient.

A range of sample solution concentrations in dioxane were made and their absorbance

measured at 455 nm. A plot of absorbance against the area for the sensor was done. Sample quantum yield was calculated in comparison to quinine sulphate dihydrate ($C_{40}H_{54}N_4O_{10}S$) from AnaSpec contained in 0.1M perchloric acid (Nawara & Waluk 2019) as a fluorophore standard of known quantum yield. The Φ of $C_{40}H_{54}N_4O_{10}S$ is known to be 0.546 (excitation. = 3.1×10^{-7} m, emission. = 4.55×10^{-7} m). (Wang *et al*., 2019). Compound **3** was allowed to interact with excess fluoride ions in dioxane for 1 minute before the fluorescence intensity could be measured.

Paper Disc Assays

Whatman® qualitative filter paper, Grade 1, circles, diameter 25 mm, was punched into small disks to make paper discs. In a 1:3 THF: DCM solvent, a 2 mM solution of compound (**3**) was prepared. After that, the paper disks were soaked in this solution and allowed to dry. To detect aqueous fluoride, the pre - treated filter paper discs were soaked for 5 seconds in an un-buffered aqueous 2 mM cetyltrimethylammonium bromide, CTAB, and allowed to dry for 5 minutes. Using a handheld Ultraviolet light source (UVGL-58 from UVP), the fluorescence on the paper discs were recorded below 3.65×10^{-7} m.

Selectivity Assay

An artificial aquifer with twice NaF concentration to be used in the test (2 x (20,40,50, 60,80,100) was made. Each aquifer concentration was further diluted in a 1:1 (v/v) by adding 10 mM acetate comprising 2 millimolar cetyltrimethylammonium bromide to maintain the pH at 4.8. The fluorescence of this solution was immediately measured using compound (**3**) impregnated paper discs.

RESULTS AND DISCUSSION

Spectral Information on Compound 3

The ^{1}H NMR (500 MHz, DMSO-d_6) spectrum showed different multiplicities with aliphatic protons resonating 7.79 (s, 1H), 2.56 (s, 9H), 1.84 (s, 6H). While the aromatic protons at δ 7.72 (s, 1H), 6.89 (d, J = 8.9 Hz, 1H), 6.83 (dd, J = 8.9, 2.3 Hz, 1H). The ^{13}C NMR (500 MHz, DMSO-d_6) δ 165.02 , 163.92 , 157.94 , 155.58 , 135.38 , 129.32 , 121.68 , 118.42 , 115.24 , 114.78 , 111.02 , 102.83 , 96.45 , 30.70 , 28.24 , 18.36. The^{1}H-^{1}H COSY (500 MHz, DMSO-d_6) ^{1}H–^{1}H coupling was observed between δ 7.72 and δ 6.89 while two-bond coupling (^{1}H–C–^{1}H) were between δ 6.83 and δ 6.89. The multiplicity pointed to the fact that the proton directly attached to the benzene ring at δ 6.85 is coupled to the two others at δ 7.72 and δ 6.83, thus the signal at δ 6.85 is a double duplet. The aromatic proton at δ 7.72 only shows coupling with another at 6.85 hence is a duplet. The non-aromatic protons at δ 1.84, δ 2.56 and δ 7.79 all show no coupling and appear as singlets. The Mass spectrum revealed an $M^+ + 1$ at 330.3. A single diode array peak at 2.92 retention time on this compound confirms its purity.

Fluorescence Properties

The samples' fluorescence intensity was recorded using an excitation wavelength of 329 nm and an emission of 362 nm. Compound (**3**) therefore**,** registered a stokes shift of 33 nm (Figure4). The average change in fluorescence intensity of three replicates with increasing fluoride ionic strength was recorded. The figure shows that the fluorescence intensity linearly corellates with increase in fluoride concentration, reflecting a 1:1 stoichiometric ratio between fluoride ionic strength and concentration of compound (**3**). The fluorescence intensity at 200s for compounds calculated by substituting time in seconds into the linear equation (y = -0.0106x + 3.6443) in figure 5 yielded a 1.52 AFU.
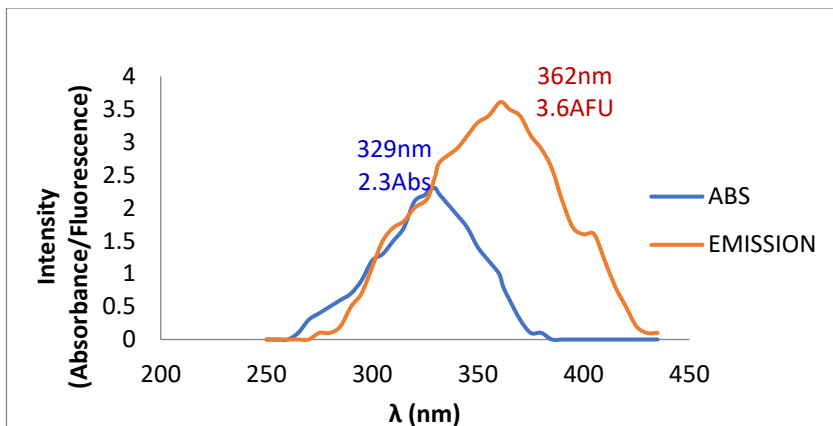
Figure 4: Excitation and emission spectra of compound **3** (200 µM) in F⁻ free solution.

Selectivity Studies and Limit of Detection

An investigation on the Fluoride limit of detection by compound **3** in TBAF verified the capability to detect TBAF dosages as low as 0.19 µM (3.61×10^{11} mgL⁻¹). The response of sensor **3** to diminishing NaF concentration in a 1:1 (v/v) solution of dioxane: H_2O gave a 8.5 µM (3.79×10^{10} mgL⁻¹) limit of detection. This is clearly much lower than the present WHO guiding principle for drinking water fluoride concentration which has been set at ≤ 789.4 µM (1.5 mgL⁻¹). The response of compound (**3**) as a fluoride sensor in the existence of other competing anions; chloride, bromide, iodide, nitrate and sulfate did not reveal any direct competition with any of the tested anions (Figure 6). The results undoubtedly show that environmentally relevant anions present in groundwater have negligible interference to fluoride sensing by compounds (**3**).
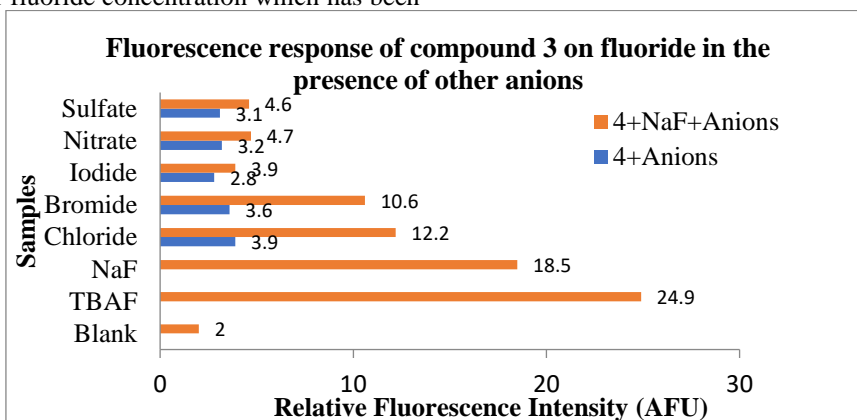

Figure 6: Selectivity of compound **3** (20 µM) for fluoride in the existence of other anions.

The rates of reactions for each of the compound **3** was obtained for each of the set concentrations by using equation (ii) after making a plot of fluorescence intensity increase with time (Figure 5) and substituting the values into equation (ii).

Fluorescence = $1 - \exp(-k_{obs}t)$ ....(ii)

Where;
t = time in minutes.
k_{obs}, = pseudo-first-order rate constant

A plot of k_{obs} against [NaF] was used to calculate the second-order rate constant equation (iii).

$k_{obs} = k_2[NaF]$ ....(iii)

Where;

k_2 = second-order rate constant.

The 2nd order rate constant was established to be 1.4 x10 M^{-1}min^{-1} demonstrating the ability of compound **3** to rapidly detect the presence of aqueous fluorides in portable water as compared to a range of 0.54 M^{-1}min^{-1} to 116 M^{-1}min^{-1} for most fluoride sensors.
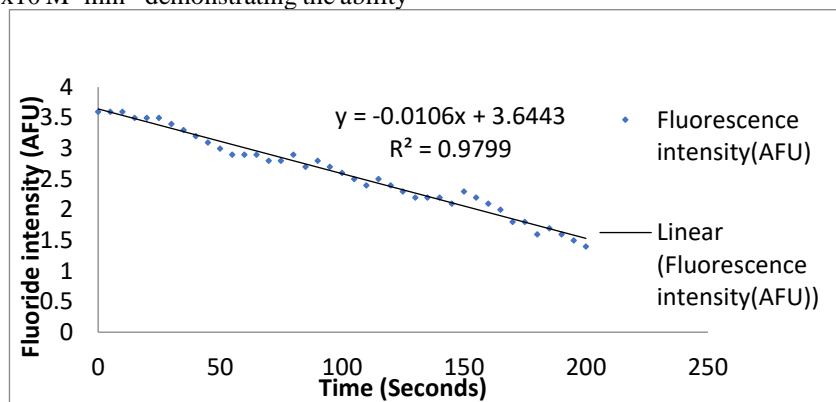

Figure 7: Time-dependent fluorescence intensity of compound 3 fluoridated solutions.

Quantum Yield

The quantum yield of compound **3** was higher than the standard (quinine sulfphate) at 0.72 and 0.54, respectively. This value was calculated by measuring the integrated Fluorescence intensity of sample in dioxane (refractive index η= 1.42) against quinine sulphate in 0.1 M perchloric acid (refractive index η= 1.33) as standard (Figure7). This indicates that compound **3** has a higher efficiency of photon emission than Quinine sulphate.
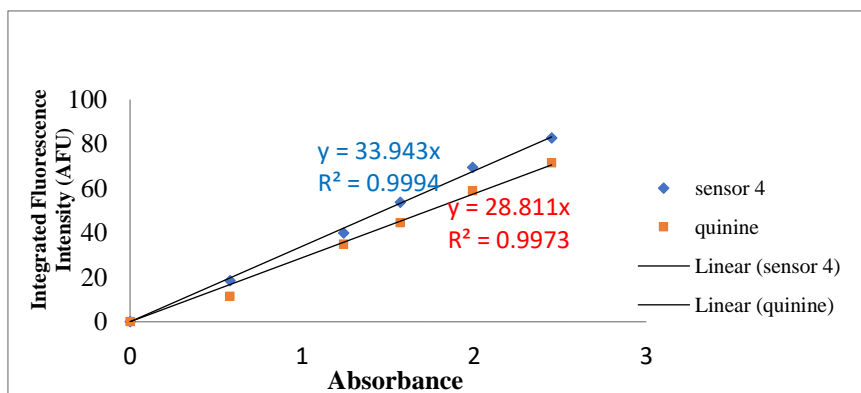

Figure 8: Plot of integrated fluorescence intensity of compound (**3**) against the corresponding absorbance for the standard (quinine sulphate).

Paper Disc-Based Sensing of Fluoride in Aqueous Samples

Since we target portable water, we envisioned the use of test paper discs as cheap and therefore can be easily accessible fluoride probes. This can be done by monitoring the fluorescence changes in the probe. The addition of TBAF to a solution of compound (**3**) resulted in vivid changes in both excitation and emission wavelengths, as desilylation occurs (Figure 9). Increasing fluorescence is observed with increasing TBAF concentration.
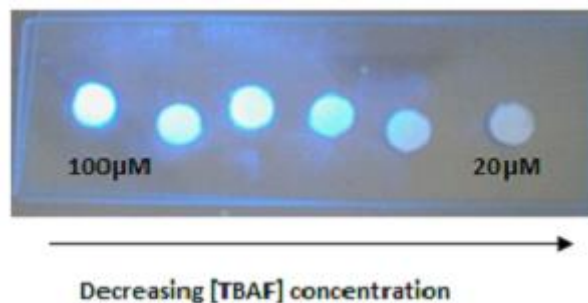
Figure 9: Fluorescence of paper discs containing the sensor with decrease in tbaf concentration.

The paper disc-based test was indeed sensitive enough to detect fluoride when other competing anions were present. These findings suggest that the 7-O-tert-butyldimethylsylyl-2-(hydroxyimino)-4-methyl-2H-chromene-3-carbonitrile scaffold has the capacity to be a robust platform for the design of customized fluoride sensing scaffolds. The paper disc-based test mentioned above may be combined with hand-held lateral fluorescence viewers to allow for faster fluoride content analysis.

CONCLUSION

Finally, 7-O-tert-butyldimethylsylyl-2-(hydroxyimino)-4-methyl-2H-chromene-3-carbonitrile was successfully synthesized. Its adaptability as a probe for the development of exceedingly responsive and discriminating scaffold for aqueous fluoride analysis was demonstrated. The potential of this dye to be utilized in aqueous fluoride detection is huge. This shall allow for simple fluoride analysis at concentrations well below the WHO recommendations.

Because of the low solubility of 7-O-tert-butyldimethylsylyl-2-(hydroxyimino)-4-methyl-2H-chromene-3-carbonitrile in water, a paper disc-based fluoride test in water was developed. This probe can be theoretically used for cheap fluoride content evaluation. Finally, this research offers a flexible, cheap medium for analyzing fluoride in small as well as large water samples.

References

Akimov, O. Y. and Kostenko, V. O. (2020). Role of NF-KB Transcriptional Factor Activation during Chronic Fluoride Intoxication in Development of Oxidative-Nitrosative Stress in Rat's Gastric Mucosa. *Journal of Trace Elements in Medicine and Biology* 61:126535. doi: 10.1016/j.jtemb.2020.126535.

Cao, X., Na, Z., Haiting, L., Aiping, G., Aiping, S. and Yongquan, W. (2018). 4-Nitrobenzene Thiourea Self-Assembly System and Its Transformation upon Addition of Hg^{2+} Ion: Applications as Sensor to Fluoride Ion. *Sensors and Actuators B: Chemical* 266:637–44. doi: 10.1016/j.snb.2018.03.188.

Helte, E., Carolina, D. V., Kippler, M, Wolk, A., Karl, M. and Åkesson, A. (2021). Fluoride in Drinking Water, Diet, and Urine in Relation to Bone Mineral Density and Fracture Incidence in Postmenopausal Women. *Environmental Health Perspectives* 129(4):EHP7404, 047005. doi: 10.1289/EHP7404.

Kabir, H., Ashok, K. G. and Subhasish, T. (2020). Fluoride and Human Health: Systematic Appraisal of Sources, Exposures, Metabolism, and Toxicity. *Critical Reviews in Environmental Science and Technology*

50(11):1116–93. doi: 10.1080/10643389.2019.1647028.

Keesari, T., Diksha, P., Annadasankar, R., Uday, K. S., Ajay, J., Manveer, S. and Jain, S. K. (2021). Fluoride Geochemistry and Exposure Risk Through Groundwater Sources in Northeastern Parts of Rajasthan, India. *Archives of Environmental Contamination and Toxicology* 80(1):294–307. doi: 10.1007/s00244-020-00794-z.

Kruse, A. B., Nadine, S., Viktoria, K. K., Cornelia, F., Annette, A., Annette, W., Elmar, H., Kirstin, V. and Ali, A. (2021). Long-Term Use of Oral Hygiene Products Containing Stannous and Fluoride Ions: Effect on Viable Salivary Bacteria. *Antibiotics* 10(5):481. doi: 10.3390/antibiotics10050481.

Liese, D. and Gebhard, H. (2018). Rotations in Excited ICT States - Fluorescence and Its Microenvironmental Sensitivity. *Israel Journal of Chemistry* 58(8):813–26. doi: 10.1002/ijch.201800032.

Magri, D. C. (2021). Logical Sensing with Fluorescent Molecular Logic Gates Based on Photoinduced Electron Transfer. *Coordination Chemistry Reviews* 426:213598. doi: 10.1016/j.ccr.2020.213598.

Mizuta, T., Kenji, S., Tatsuro, E. and Hideaki, H. (2021). Lipophilic Fluorescent Dye Liquids: Förster Resonance Energy Transfer-Based Fluorescence Amplification for Ion Selective Optical Sensors Based on a Solvent Polymeric Membrane. *Analytical Chemistry* 93(9):4143–48. doi: 10.1021/acs.analchem.0c05007.

Mohanasundaram, D., Gujuluva, G. V. K., Senthuran, K. K., Balaji, M., Ramachandran, P. R., Jegathalaprathaban, R. and Gandhi, S. (2020). Turn-on Fluorescence Sensor for Selective Detection of Fluoride Ion and Its Molecular Logic Gates Behavior. *Journal of Molecular Liquids* 317:113913. doi: 10.1016/j.molliq.2020.113913.

Nawara, K. and Jacek, W. (2019). Goodbye to Quinine in Sulfuric Acid Solutions as a Fluorescence Quantum Yield Standard. *Analytical Chemistry* 91(8):5389–94. doi: 10.1021/acs.analchem.9b00583.

Song, Y. and Junhewk, K. (2021). Community Water Fluoridation: Caveats to Implement Justice in Public Oral Health. *International Journal of Environmental Research and Public Health* 18(5):2372. doi: 10.3390/ijerph18052372.

Srivastava, S. (2020). Fluoride in Drinking Water and Skeletal Fluorosis: A Review of the Global Impact. 7.

Ullah, U., Murtaza, H. S., Daniyal, G., Falak, S. and Cheema, M. I. (2021). Fluoride Detection in Drinking Water Using Evanescent Fiber Cavity Ring Down Spectroscopy. 6.

Wang, Y., Yaxin, M., Jie, H., Qianfen, Z. and Yongnian, N. (2019). Rapid, One-Pot, Protein-Mediated Green Synthesis of Water-Soluble Fluorescent Nickel Nanoclusters for Sensitive and Selective Detection of Tartrazine. *Spectrochimica Acta Part A: Molecular and Biomolecular Spectroscopy* 214:445–50. doi: 10.1016/j.saa.2019.02.055.

Wu, N., Li-Xia, Z., Chun-Yu, J., Ping, L., Yulong, L., Ying, F. and Fei, Y. (2020). A Naked-Eye Visible Colorimetric and Fluorescent Chemosensor for Rapid Detection of Fluoride Anions: Implication for Toxic Fluorine-Containing Pesticides Detection. *Journal of Molecular Liquids* 302:112549. doi: 10.1016/j.molliq.2020.112549.

Xu, X., Xiangheng, N., Xin, L., Zhaohui, L., Dan, D. and Yuehe, L. (2020). Nanomaterial-Based Sensors and Biosensors for Enhanced Inorganic Arsenic Detection: A Functional Perspective. *Sensors and Actuators B: Chemical* 315:128100. doi: 10.1016/j.snb.2020.128100.

Yeung, M. C., Ben, W. C. and Vivian, W. Y. (2014). Anion Binding Properties of Alkynylplatinum (II) Complexes with Amide-Functionalized Terpyridine: Host-Guest Interactions and Fluoride Ion-Induced Deprotonation. *ChemistryOpen* 3(5):172–76. doi: 10.1002/open.201402019.